Rotational and Translational Diffusion of a Rodlike Virus in Random Coil Polymer Solutions

Randy Cush,[†] Paul S. Russo,[*,†] Zuhal Kucukyavuz,[‡] Zimei Bu,[§] David Neau,[†] Ding Shih,[||] Savas Kucukyavuz,[‡] and Holly Ricks[†]

Departments of Chemistry and Biochemistry, Louisiana State University, Baton Rouge, Louisiana 70803, Department of Chemistry, Middle East Technical University, Ankara, Turkey 06531, and Department of Molecular Biophysics, Yale University, New Haven, Connecticut 06520-8114

Received January 14, 1997; Revised Manuscript Received June 9, 1997[⊗]

ABSTRACT: Depolarized dynamic light scattering was used to measure the translational and rotational diffusion of tobacco mosaic virus, TMV, in aqueous solutions of dextran (M ∼505 000). TMV is an electrically charged, nucleoprotein assembly with the shape of a stiff, rigid rod. Dextran is an uncharged, flexible carbohydrate polymer. The TMV was held at a fixed, dilute concentration (0.5 mg/mL), while the concentration of dextran spanned both dilute and semidilute regimes (0−14.5% by weight). There was no evidence of phase separation or strong aggregation of the TMV particles in the presence of the dextran. The TMV particles dominated the depolarized scattering at all dextran concentrations. The angular variation of the decay rates of the autocorrelation functions always followed the form expected for symmetric top molecules in the absence of translational−rotational coupling. Nevertheless, translational and rotational motions are almost surely coupled in most dextran-containing solutions. The apparent translational and rotational diffusion rates decreased with added dextran, but not exactly according to the rise in macroscopic solution viscosity. A transition occurred at about 6.5% dextran. Beyond this concentration, pronounced failures of the continuum (Stokes−Einstein) relation between diffusion and viscosity were found. Translational diffusion continued more rapidly than expected on the basis of the macroscopic viscosity, while rotational diffusion fell sharply below expectation. The quotient D_r/D_t of rotational and translational diffusion, which presumably cancels effects due to viscosity, also dropped suddenly above the transition point. These findings are consistent with a sudden onset of topological constraints to rotational motion of the TMV, without onset of severe constraints to translational motion. Temperature dependent studies showed that either the solution or the solvent viscosity can describe translation and rotation fairly well, at least at concentrations below the transition. Energies of activation for translational and rotational diffusion of TMV were similar and not strongly dependent on dextran concentration in this regime.

Introduction

The nature of entanglements in polymer solutions remains a difficult problem. At the macroscopic level, gradual increases in viscosity may be expected once entanglements begin to form, but the effects on motion at small distance scales are less certain. A popular approach is to monitor changes in the diffusion of some type of probe as the polymer concentration is raised. Such probe diffusion studies are also related to important processes, ranging from organelle transport in living cells to the drying of paints. Linear and star polymers have been used as probes, in addition to colloidal particles and molecules spanning a wide size range.[1−13] Despite the enormity of this enterprise, there is little information about the dynamic behavior of rodlike probes. Also, comparatively little attention has been paid to rotational diffusion of the probes.[14,15] These omissions have practical consequences because production of advanced rod/coil composite materials relies on precursor solutions. The stability and alignment of the rods, and therefore the success of the materials, depend critically on translational and rotational mobility.

One of the most powerful methods for diffusion measurement is dynamic light scattering, DLS. Its application to probe diffusion requires that the probe scatters much more strongly than the polymer matrix. The ideal limit of zero matrix scattering is reached when the matrix polymer has the same refractive index as the solvent.[16,17] Such isorefractive pairs do not exist for aqueous systems, which are otherwise desirable because of the strong reduction of electrostatic attractions afforded by a high dielectric constant.

This paper describes the use of *depolarized* DLS to follow the translational and rotational diffusion of Tobacco Mosaic Virus, TMV, through aqueous solutions of dextran, which is effectively invisible in the depolarized scattering experiment. TMV is an essentially rigid rod of length $L = 300$ nm and diameter $d = 18$ nm.[18−20] Dextran is a typical random coil polymer.[21,22] The experiments demonstrate the potential utility of rodlike probes and provide some new insights into the importance of hydrodynamic interactions relative to topological constraints in solution.

Light Scattering Background

The geometry of the light scattering experiments discussed here is either Uv (detection of all light scattered from a vertically polarized incident beam) or Hv (detector horizontal, incident light vertical). Since the depolarized signal is small,[23] the Uv scattering closely resembles the Vv signal (incident light and detector both vertical). The intensity autocorrelation function for a monodisperse scatterer at sufficiently low scattering vector, **q**, is given by

$$g^{(2)}(t) = 1 + f|g^{(1)}(t)|^2 \quad (1)$$

* To whom communications should be addressed.
[†] Department of Chemistry, Louisiana State University.
[‡] Middle East Technical University.
[§] Yale University.
[||] Department of Biochemistry, Louisiana State University.
[⊗] Abstract published in *Advance ACS Abstracts,* August 1, 1997.

S0024-9297(97)00032-6 CCC: $14.00

where f is an instrumental parameter, $0 < f < 1$, related mostly to spatial coherence. The electric field autocorrelation function, $g^{(1)}(t)$, is

$$g^{(1)}(t) = \exp(-\Gamma t) \tag{2}$$

where Γ is a decay rate. Experiments in the Uv geometry sense mostly translational diffusion and are characterized by

$$\Gamma_{Uv} = q^2 D_t \tag{3}$$

where D_t is the translational diffusion coefficient and q is the scattering vector magnitude ($q = 4\pi n \sin(\theta/2)/\lambda_o$ where n is the solution refractive index, θ is the scattering angle, and λ_o is the incident light wavelength *in vacuo*). It will be demonstrated that the present experiments are in the low concentration limit for TMV, so that the differences between mutual and self-diffusion coefficients may be ignored. At sufficiently high q, a rotational component adds additional exponential terms to the relaxation of the Uv correlation function.[24,25] This can be very useful in dilute solutions, especially for rodlike structures that do not depolarize much light.[26] In the present experiments, the multiple exponential Uv scattering from TMV at high q would combine with the significant Uv scattering from the dextran matrix to give a correlation function that would be impossibly difficult to interpret. It would even be hard to interpret the low-q results.

The situation for Hv scattering is better, since dextran has almost zero depolarized signal. A cylindrically symmetrical, optically anisotropic, monodisperse and inflexible scatterer like intact TMV has a depolarized decay rate with q-dependent and q-independent terms:[24]

$$\Gamma_{Hv} = q^2 D_t + 6D_r \tag{4}$$

where D_r is the end-over-end rotational diffusion coefficient. A series of measurements at different q yields both D_t and D_r. Equation 4 ignores coupling of translation and rotation, which arises because hydrodynamic friction is greater for sideways motions than for longitudinal motions of the rod.[25,27−30] The importance of this effect can be gauged through a coupling parameter $\gamma = q^2 \Delta D_t / D_r$ where ΔD_t is the anisotropy in translational diffusion. Equation 4 is valid for small γ, that is, if the rod reorients many times while diffusing a distance comparable to q^{-1} or if there is little anisotropy so that the rate of translational diffusion varies little with orientation. For TMV in the absence of dextran, and for the q values used in this study, we have $1 < \gamma < 7$. Even higher values may be reached in the dextran matrix, but the consequences are not entirely clear. Zero and Pecora[27] showed that, for $\gamma < 10$, the single exponential decay of eq 4 is split into four exponentials, with q-dependent amplitudes and decay rates involving ΔD and D_r. Though intended for semidilute binary solutions of rods, ref 27 is actually more appropriate for the present case of a single rod diffusing in an entangled matrix, unfettered by thermodynamic interactions with other rods. This does not imply that anything like four cleanly separated exponentials should be expected experimentally. The theory of Maeda[31] for the Hv scattering of semidilute rods, including thermodynamic interactions, would be inappropriate in the present situation because the rods are held at a concentration where they do not interact with each other.

Materials and Methods

Tobacco plants grown from seeds (Ward Scientific) were infected at about 15−30 cm height with the U1 strain of TMV. The plants were harvested at a typical height of 1 m, and TMV was isolated by a procedure similar to that of Boedtker and Simmons.[19] Details appear in the Supporting Information. TMV was stored at 4 °C at a concentration of about 30 mg/mL in a 0.01 M phosphate buffer, pH 7.5. Dilutions to measurement concentrations were performed with dedusted 0.01 M phosphate buffer (with 3 mM NaN_3 to prevent bacterial growth). TMV concentrations were determined using an absorbance of 3000 $cm^2\ g^{-1}$ at 260 nm.[32] Dextran (Sigma Cat. No. D-1037, lot 25H0440) had an advertised weight-average molecular weight of $M_w = 505\,000$. This value was checked by static light scattering experiments, which also gave an apparent radius of gyration (the root of the z-average of the squared radius of gyration) of 36 ± 2 nm. The measured intrinsic viscosity was $[\eta] = 0.415 \pm 0.006$ dL/g. The dextran was dedusted by filtering through a 0.1 μm Millipore Millex filter into clean acetone. After vacuum drying, dextran stock solutions in the just-described phosphate buffer were prepared directly in DLS cells, which were simple 13-mm test tubes surface-treated with chlorotrimethylsilane to facilitate cleaning. These solutions were heated mildly and equilibrated several weeks if necessary before adding TMV. Other dextran concentrations were prepared from these solutions by weighing in aliquots of 0.5 mg/mL TMV in buffer. Samples were refrigerated when not in use.

The DLS apparatus was similar to the one described[33] for zero-angle depolarized scattering but was used at finite angles only. An argon ion laser supplied about 250 mW at $\lambda_o = 514.5$ nm. Each DLS cell was elevated slightly so that the incident light passed through the cell near the intersection of the cylindrical surface and the rounded bottom. In this way, the back-reflected beam could be separated from the forward going beam, and did not have to be absorbed. The separation, equal to several beam widths, was adjusted using the detector's viewing port, which enables the user to see exactly the light that will be measured on the EMI-9863 photomultiplier tube. An ALV-5000 multibit correlator was used to obtain the correlation functions, sometimes as the average of several short runs. Discrimination against very occasional dust was achieved by the ALV-5000 software or by our own interactive software. Measurements were made at 4 or 5 scattering angles corresponding to the condition $2.5 < qL < 5.6$ or 7. At the very highest dextran concentrations, mild centrifugation of the samples was rewarded with slightly improved consistency, but the data trend was not affected and centrifugation was usually not used. Dextran-containing samples were measured with a 514.5-nm line filter in the detector to remove a very slight trace of fluoresced light, probably due to an unknown impurity. The samples exhibited no thermal lensing.

Viscosities were measured with a Brookfield LVTDCP cone and plate viscometer calibrated with water. At elevated temperatures, the measurement chamber was fitted with wet sponges to prevent evaporation and the spindle assembly was separately heated to improve temperature uniformity. When possible, viscosities were extrapolated to zero rate of shear. The shear rate dependence was modest in the measured range (2.25−450 s^{-1}). Temperatures were controlled to ±0.05 °C (light scattering) or ± 0.02 °C (viscosity) and calibrated against a mercury thermometer traceable to the National Institute of Standards and Technology.

Small angle X-ray scattering (SAXS) measurements were used to estimate the correlation lengths of the dextran solutions. The X-ray source was a Rigaku RU-300 rotating anode generator operating at 50 kV and 180 mA, producing 1.5 Å Cu Kα radiation. The beam was pinhole collimated with an incident beam diameter of 1.2 mm. A two-dimensional multiwire detector with 256 × 144 pixels and a sensitive area of 290 × 299 mm was placed 2.3 m from the sample holder. The scattering vector magnitude q ranged from 0.010 to 0.36

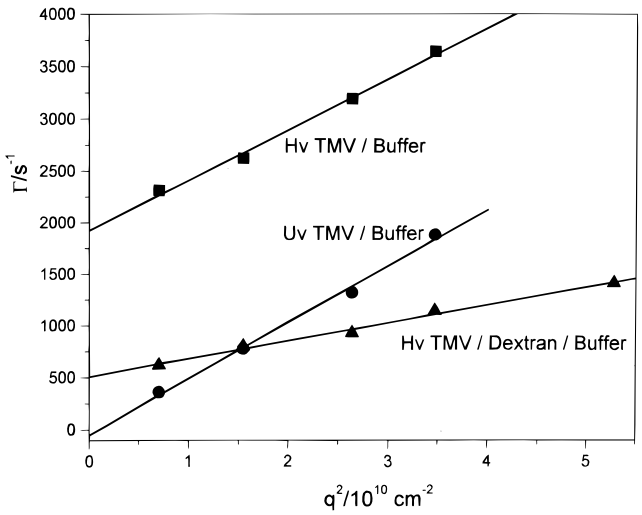

Figure 1. Dependence of Γ_{Hv} (squares) and Γ_{Uv} (circles) on squared scattering vector magnitude for TMV in buffer (c = 0.2 mg/mL). Triangles show Hv behavior for TMV in 4.17 wt % dextran/buffer solution.

Å^{-1}. Two-dimensional scattering patterns were circularly averaged. Approximately 100 μL samples were transferred into 2 mm path length quartz capillary tubes. The same capillary tube was later rinsed with buffer and reused for the next sample so that the instrument factor was unchanged during the measurements. Data collection times were 1 h.

A Beckman XLA analytical ultracentrifuge was used to measure the sedimentation coefficient of the TMV. The scanning absorption optics were set to 260 nm to follow the boundary as it sedimented over a period of several hours at 6500 rpm.

Results and Discussion

Characterization of TMV in Dilute Binary Solution. The sedimentation coefficient of TMV, corrected for viscosity and density to conditions at 20 °C, was S_{20w} = 182 ± 2 S at 0.2 mg/mL. This concentration lies in the dilute regime according to Boedtker and Simmons,[19] who obtained 188 S at infinite dilution, in reasonable agreement with our result. In dilute solution, the Hv decay rate is dominated by the rotational diffusion term. Since this varies approximately as L^{-3}, depolarized DLS is a good way to detect polydispersity.[33,34] Although the TMV sedimented as a single band in the analytical ultracentrifuge, measured Hv correlation functions were not single exponential decays, even at low q where the coupling parameter γ was small. This is almost surely due to TMV fragmentation, possibly exacerbated by the presence of phosphate.[35] Variations in the integrity of the noncovalently self-assembled virus undoubtedly contribute to the poor agreement among various workers on translational and rotational diffusion of TMV. References 36 and 28 tabulate some results. When the present Hv DLS correlation functions were analyzed by the Laplace inversion program CONTIN,[37−39] a bimodal distribution of relaxation times was almost always found. The weaker, faster mode was sufficiently rapid to affect the average decay rate that would be measured by cumulant analysis.[39,40] The stronger, slower decay mode increased linearly with q^2, as shown in Figure 1. The intercept leads to D_r = 318 ± 2 s^{-1} at 24.6 °C. Correcting to 20 °C gives D_{r20w} = 281 ± 2 s^{-1} in good agreement with the value 294 s^{-1} computed for L = 300 nm and d = 18 nm from Broersma's equations.[41−44] The expressions of Tirado *et al.*[44,45] predict D_r = 316 s^{-1}. Our D_r value is on the low end of the observed spectrum, which ranges up to about 360 s^{-1}. Third-order cumulant fits to extract the average decay rate would place us nearer the typical values, but given the known problems with TMV fragmentation, it is felt that the primary decay mode should be used alone. Figure 1 also shows Uv results in pure water. The slope is almost identical to that of the Hv experiments. Extrapolation of Uv and Hv slopes to zero concentration gives D_t = (5.0 ± 0.4) × 10^{-8} cm^2 s^{-1} at 24.6 °C or D_{t20w} = (4.4 ± 0.35) × 10^{-8} cm^2 s^{-1}. This significantly exceeds the values often reported in the literature (ca. 3.4 × 10^{-8} cm^2 s^{-1}) but is only about 5% greater than the result of Wilcoxon and Schurr [(4.19 ± 0.10) × 10^{-8} cm^2 s^{-1}] who discuss the deficiencies of the older determinations.[28] The 5% difference between this study and ref 28 may be attributed to either polydispersity or data handling. Since our measurements were not extrapolated to the very low q regime, end-over-end tumbling may have made a weak contribution that is not resolved in the CONTIN analysis. Nonetheless, as for rotation, the present D_t value agrees reasonably well with the Broersma or Tirado *et al.* expectations, which are 4.02 × 10^{-8} and 4.52 × 10^{-8} cm^2 s^{-1}, respectively. The TMV molecular weight can be obtained from sedimentation−diffusion[46] as $M = SRT/D_t(1 - \rho v)$ where R is the gas constant, ρ is solvent density, and v is the partial specific volume. Taking v = 0.73 mL/g[47] and using our results for S and D_t gives M = 37.5 × 10^6, which is a typical value.[19]

Establishing Appropriate Conditions for TMV as a Probe. The decay rate distribution was almost always bimodal in ternary TMV/dextran/buffer preparations, as it was for the dilute binary solutions. The stronger, slower peak was used and the more rapid, weaker peak not considered further. Fairly large values of the coupling parameter γ were expected, but the decay rate from the main CONTIN peak was always consistent with eq 4, as shown in Figure 1 for 4.17% dextran. Neverthless, out of respect for the translational−rotational coupling issue, we consider both D_r and D_t to be *apparent* quantities. In Figure 1, both are clearly reduced, relative to buffer, by the addition of dextran.

TMV is to be used as a *dilute* probe, but there are limits. Despite its large mass and extended shape (L/d ≈ 17) TMV depolarizes weakly,[23] reflecting the globular nature of its *ca.* 2130 protein subunits. Dextran will depolarize even less efficiently on a per molecule basis but will sometimes be present at elevated concentrations. A compromise must be reached between the need for TMV to be dilute and the need for it to overwhelm the dextran scattering. Figure 2 shows the concentration dependence of D_r and D_t in buffer. The concentrations are near or below the theoretical onset[48−50] of semidilute behavior for binary rods—i.e., a number density of about $1/L^3$. For TMV, this corresponds to a concentration of about 2.5 mg/mL. A TMV concentration of 0.5 mg/mL was selected for the TMV/dextran studies, well below the theoretical limit and clearly indistinguishable from measurements at still lower concentrations. The electrophoretic studies of Deggelmann *et al.*[51] also place the selected concentration in the dilute regime for solutions with added salt. At the selected concentration, the Hv signal was strong enough that good correlation functions were obtained in about 5 min with only very rare interference from dust. For the most concentrated dextran solution, the Hv TMV scattering exceeded that from dextran alone by a factor of 20−40 depending on scattering angle. Figure 3 shows

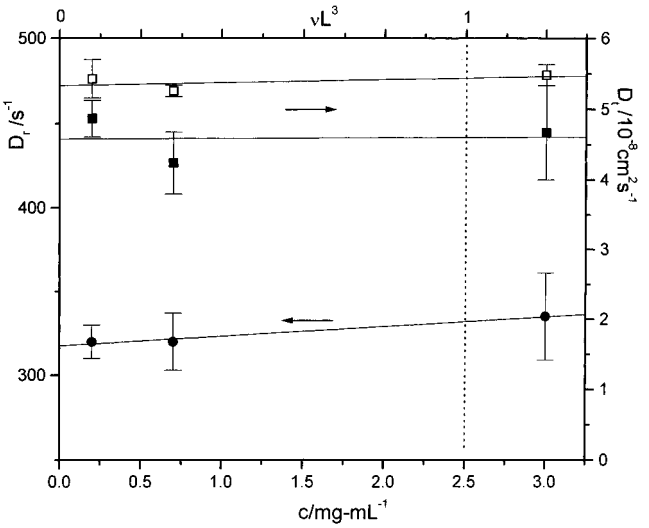

Figure 2. Dependence of D_r (●) and D_t (Hv (■) and Uv (□)) upon TMV concentration. The vertical dashed line shows the overlap concentration, where there is one rod per volume L^3.

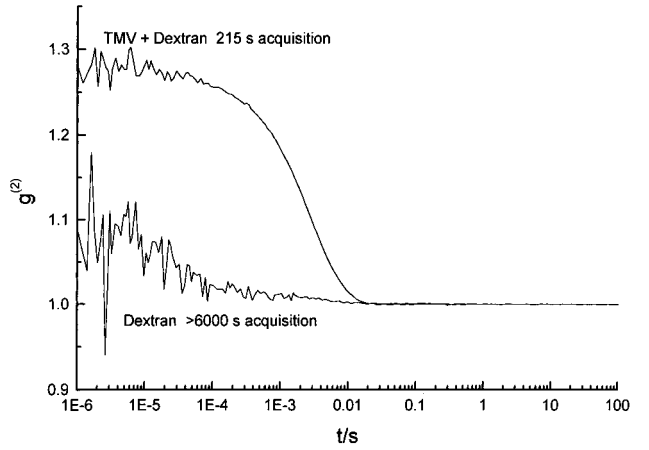

Figure 3. Hv correlation functions for 14.5 wt % dextran with and without added 0.5 mg/mL TMV, measured under identical optical conditions but using different acquisition times, indicated.

depolarized correlation functions for dextran and TMV/dextran collected using identical optical settings. The signal from the dextran is adequately suppressed and actually rather difficult to measure at all, despite a long acquisition time compared to that used for the TMV-containing solution. The reduced coherence compared to the TMV-containing solution implies that the depolarized scattering from dextran is approximately as intense as that arising from the buffer.[52,53]

The next issue is the stability of TMV in dextran solutions. One does not expect rodlike and random polymers to be very compatible,[54] though the usual segregation into phases rich in rods or coils would be opposed by charge−charge interactions among the TMV particles. Considering also the low TMV concentrations, it is not too surprising that there were no signs of phase separation. To test for dextran-induced TMV aggregation, the angular variation of depolarized intensity can be converted to the radius of gyration.[55] On the basis of somewhat imperfect[56] intensity measurements of this type, severe aggregation of the TMV particles can be ruled out, even at the highest dextran concentration. If any aggregation did occur, it was rapid since samples were stable for more than one month after preparation.

Effect of Dextran Concentration. Having established the quality of the TMV and appropriate probe diffusion

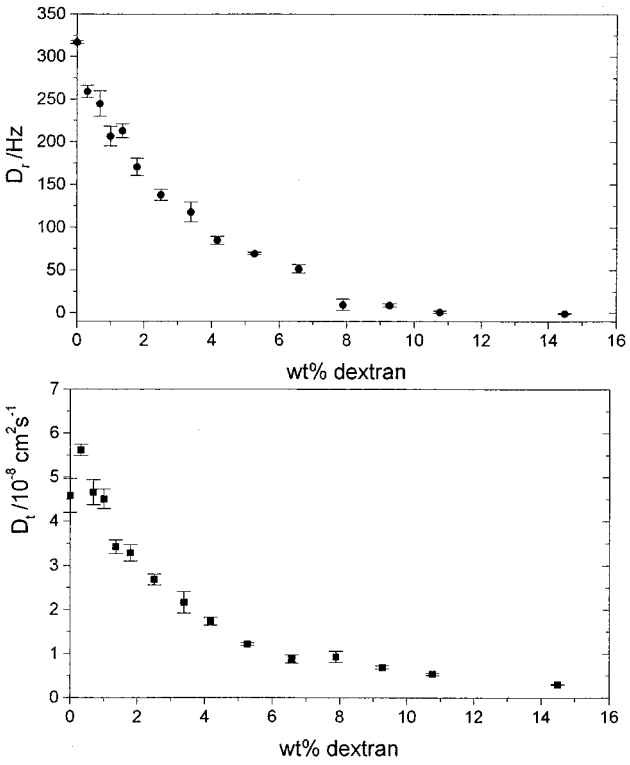

Figure 4. Dependence of rotational (top) and translational (bottom) diffusion coefficients upon dextran concentration.

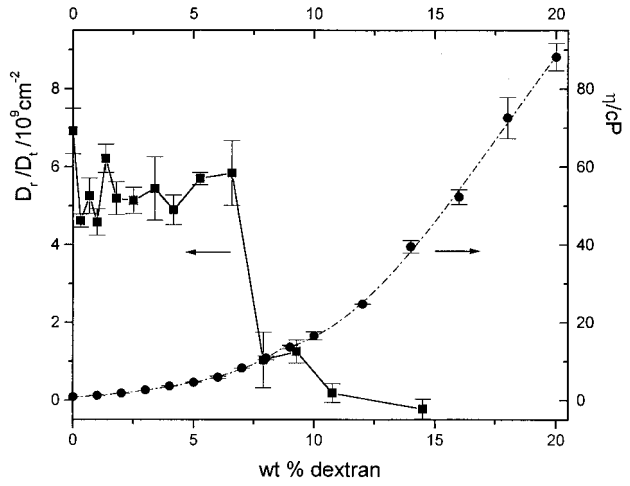

Figure 5. Dependence of the quotient of TMV rotational and translational diffusion coefficients (left scale) and dextran shear viscosity (right scale) upon dextran concentration. The dashed line through the viscosity curve represents a polynomial fit, performed in two stages; see text.

conditions, we may move ahead to the central issues. Figure 4 shows the dependence of the apparent D_r and D_t upon added dextran. Above about 10% dextran, it is no longer possible to measure D_r reliably (the intercept of Γ_{Hv} vs q^2 plots is within error of zero). There is no such problem with D_t. In Figure 5, the quotient of rotational and translational diffusion appears. A level function of added dextran at low concentrations, presumably because D_t and D_r are both approximately inversely proportional to solution viscosity, the quotient falls dramatically above about 6.5% dextran. The sudden reduction signals the appearance of a very significant constraint to TMV rotation. The dextran overlap concentration, defined as the inverse intrinsic viscosity, occurs at a much lower value, about 2.5%,

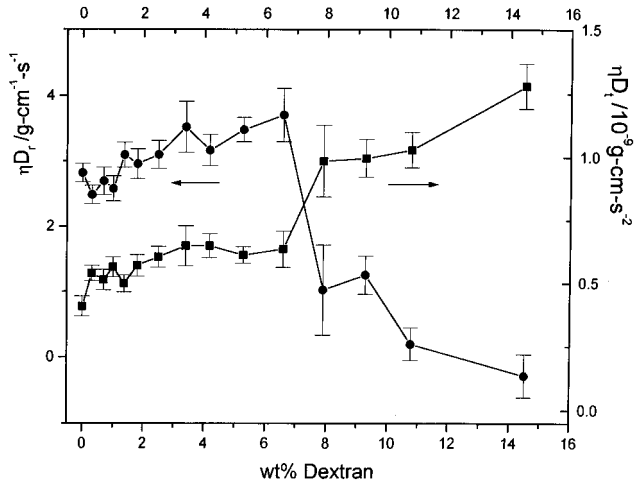

Figure 6. Product of solution viscosity and rotational diffusion (circles) and of solution viscosity and translational diffusion (squares) as a function of added dextran.

while viscosity of the solutions does not build rapidly until a somewhat higher concentration, about 10%. What rotation occurs in the regime beyond the downturn is probably strongly coupled to translational diffusion, which may be increasingly reliant on motions of the rod parallel to its own axis.[48]

Closer inspection reveals that the presumed inverse relation between diffusion and solution viscosity is never strictly true, even in the more dilute dextran-containing solutions. The viscosity curve in Figure 5 was fit to two polynomials, one for concentrations below 9% and another for higher concentrations. These polynomials were used to determine, with an error of 3% or less, the viscosities at the concentrations of the DLS measurements. Figure 6 shows that the products ηD_t and ηD_r increase modestly below 6.5% dextran. The level behavior of the D_r/D_t quotient at low dextran content in Figure 5 therefore results from like positive deviations from the Stokes−Einstein continuum expectation that diffusion be inversely proportional to viscosity. There are many instances where this rule fails; see, for example, refs 57 and 58. Above 6.5% the deviations from Stokes−Einstein become pronounced for both D_r and D_t *but in opposite directions*. Rotation is now much more restrained than one would expect from the viscosity, while translational diffusion is freer than one would expect, presumably because motions parallel to the virus axis are not much affected yet.[49] The behavior of ηD_t provides additional evidence that the TMV rods have not aggregated.

The porosity of the dextran transient network can be characterized in at least two ways. The average distance between centers of mass of the dextran molecules is given by[8]

$$\xi_{cm} = (c_{dextran} N_a / M_{dextran})^{-1/3} \quad (5)$$

where N_a is Avogadro's number. A more traditional correlation length, ξ, which represents the average distance between strands of the entangled matrix,[59] can be estimated from the angular dependence of scattered intensity:

$$1/I_s(q) \sim (1 + q^2\xi^2)/I_s(0) \quad (6)$$

At the transition concentration of 6.5% dextran, $\xi_{cm} \approx$ 23 nm, while ξ from SAXS was about nine times smaller at 2.5 nm. The difference between ξ_{cm} and ξ reflects the coil overlap. If one adopts a tube viewpoint, then each TMV is surrounded by ∼13 (i.e., L/ξ_{cm}) impeding dextran molecules supplying ∼120 (i.e., L/ξ) contacts. Caution is advised in such an interpretation, since the dextran matrix may be altered locally by the presence of the TMV in ways that correlation length cannot describe. In particular, Gold *et al.* have suggested the importance of polymer depletion zones surrounding probe particles.[9,10] That is, the presence of the probe particle prevents certain matrix polymer configurations, causing an entropic penalty for polymers that approach too closely.

Phillies[2,60] has shown that stretched exponentials of the form $D = D^0 \exp(-\alpha c^\nu)$, where D^0 is the zero concentration value, can often fit plots of diffusion vs concentration. This is true even for cases where strongly positive and sudden deviations from Stokes−Einstein behavior had been observed, with scaling slopes consistent with the reptation hypothesis.[61] A hydrodynamic scaling interpretation has been developed to explain the stretched exponential behavior. Further considerations[62] suggest that solutions graduate from the hydrodynamic regime to power-law behavior, without necessarily experiencing topological entanglements. Stretched exponentials, or even simple exponentials, fit the data of Figure 4 well up to concentrations of about 6% dextran. They are ineffective after that. The remarkable feature of the present data is that positive deviations from Stokes−Einstein law for translation are accompanied by negative deviations for rotation. It is difficult to see how both modes of motion could be controlled entirely by hydrodynamic forces. Whether or not an actual tube exists, the sudden reduction in rotational diffusion seems to provide a glimpse of the transition in the character of a solution from hydrodynamic continuum (almost) to entangled transient network. Well-defined reductions in diffusion with concentration, which were again inconsistent with a stretched exponential form, were seen in self-diffusion studies of semiflexible polymers.[63] Other examples of well-defined transitions have been reported for stiff polymers.[8,27,64]

It is clear that solution viscosity does not control all aspects of mobility in the ternary TMV/dextran/buffer system. Translation persists, presumably through longitudinal motion, well after rotation has been greatly reduced. These are central concepts in topological theories of semidilute, binary rods.[49,50] Theories describing the behavior of rods in coils are less fully developed. deGennes[65] and Deutch and Pecora[66] predict that D_r depends strongly on L for rods immersed in coils and spheres, respectively. These predictions are not accessible to the present experiments with a fixed length probe. The theory of Deutch and Pecora also predicts $D_r \sim c_{matrix}^{-2/3}$. The data of Figure 4 are consistent with a somewhat more negative exponent.

Effect of Temperature. Temperature dependent experiments were motivated by the possibility that solvent and polymer viscosities may behave differently with temperature. Then it might be possible to identify which one comes closer to governing the diffusion process in the regime below the transition, where failures of the continuum expressions are not large. Some signs of damage to the TMV were evident above about 45 °C, so only a narrow temperature range is accessible. In buffer, both translational and rotational diffusion were linear in T/η_o, where η_o is the solvent

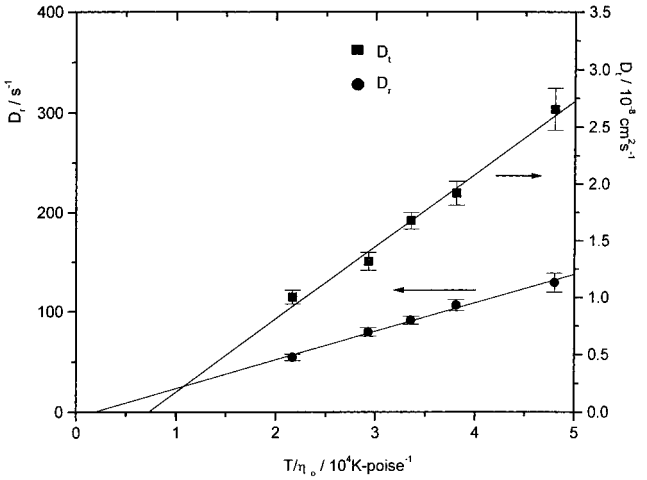

Figure 7. Rotational and translational diffusion as functions of the ratio of temperature to solvent viscosity for 4.17% dextran solution.

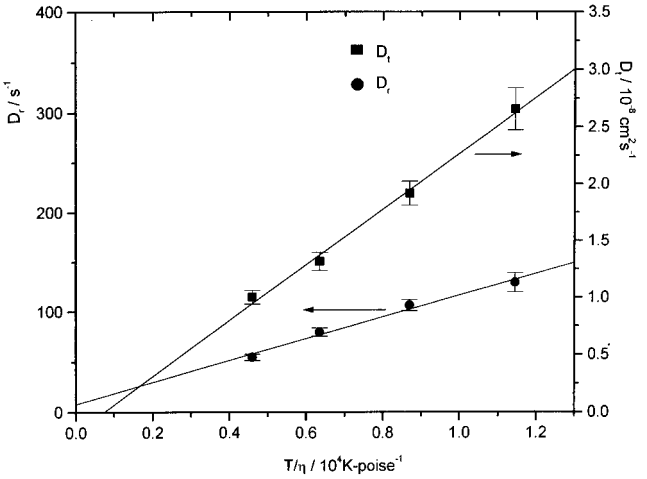

Figure 8. Rotational and translational diffusion as functions of the ratio of temperature to solution viscosity of 4.17% dextran solution.

Table 1. Activation energies for rotational and translational diffusion[a]

	buffer	1% dextran	4.17% dextran
E_t^a/kJ mol^{-1}	22 ± 1	21 ± 1	24 ± 1
E_r^a/kJ mol^{-1}	19 ± 1	21 ± 0.5	21 ± 2
E_η^a/kJ mol^{-1}	−16.5 ± 0.1[b]	−17.9 ± 0.4	−19.5 ± 0.25

[a] E_t^a defined from $D_t = D_{t,T=\infty} \exp(-E_t^a/RT)$. E_r^a and E_η^a defined similarly. [b] From tabulated water values in the range 10−45 °C.

viscosity, throughout the measured temperature range (not shown). In 4.17% dextran solution, well below the sudden transition at 6.5%, one may use either T/η_o or T/η with comparable success (Figures 7 and 8, respectively). Zero intercepts, within experimental uncertainty, are achieved only when T/η is used, but we do not believe the nonzero intercept seen when T/η_o is used to be important. Large uncertainties result from the small accessible temperature regime. Thus, the temperature dependent experiments do not clearly reveal whether solvent or solution viscosity is more appropriate. This rather indiscriminate viewpoint is confirmed by the absence of any particular trend in the energies of activation, Table 1, apart from a steady increase in magnitude for the energy of activation of viscosity with increasing dextran concentration.

Conclusion

It has been 60 years since the discovery of TMV's special solution properties, the flow birefringence and mesogenic character from which its rodlike shape was first inferred.[67] Flaws such as fragmentation notwithstanding, this ancient gift of nature still provides new insights to the behavior of rodlike polymers, in the present case surrounded by random coils. In such a situation, the mobility of the TMV is controlled mostly but not perfectly by viscosity as long as the matrix overlap concentration is not greatly exceeded. At higher concentrations, a sudden transition suggests a topological constraint for rotation, without translational diffusion being much affected. Depolarized dynamic light scattering may be a valuable addition to the arsenal of probe diffusion experiments, but proof of its general utility awaits experiments in other systems.

Acknowledgment. This work was primarily supported by NSF grants DMR-9634713, INT-9512700, and CHE-9424021. Additionally, H.R. thanks the Howard Hughes Medical Institute at Louisiana State University for Undergraduate Research. Z.B. is the recipient of NIH NRSA postdoctoral fellowship GM-17364. The analytical ultracentrifuge was purchased with NSF grant BIR-9420253. The SAXS instrument was supported by NIH Grant GM-22777E to Donald M. Engelman. We thank Professor Norimoto Murai of LSU for the TMV used to infect plants that surely benefited from the green thumb of Ms. Amanda Brown. We thank Professor Seth Fraden of Brandeis University for helpful hints about TMV isolation.

Supporting Information Available: Experimental details for the preparation of **1** and **2** (3 pages). Ordering information is given on any current masthead page.

References and Notes

(1) Lodge, T. P.; Rotstein, N. A.; Prager, S. *Adv. Chem. Phys.* **1990**, *79*, 1−133.
(2) Phillies, G. D. J. *J. Phys. Chem.* **1989**, *93*, 5029−5039.
(3) Martin, J. E. *Macromolecules* **1984**, *17*, 1279−1283.
(4) Turner, D. N.; Hallett, F. R. *Biochem. Biophys. Acta* **1976**, *451*, 305−312.
(5) Yang, T.; Jamieson, A. M. *J. Colloid Interface Sci.* **1988**, *126*, 220−230.
(6) Rymden, R.; Brown, W. *Macromolecules* **1986**, *19*, 2942−2952.
(7) Brown, W.; Rymden, R. *Macromolecules* **1988**, *21*, 840−846.
(8) Tracy, M.; Pecora, R. *Macromolecules* **1992**, *25*, 337−349.
(9) Gold, D.; Onyenemezu, C.; Miller, W. G. *Macromolecules* **1996**, *29*, 5710−5716.
(10) Gold, D.; Onyenemezu, C.; Miller, W. G. *Macromolecules* **1996**, *29*, 5700−5709.
(11) Borsali, R.; Duval, M.; Benmouna, M. *Macromolecules* **1989**, *22*, 816−821.
(12) Chu, B.; Wu, D.-Q. *Macromolecules* **1987**, *20*, 1606−1619.
(13) Pajevic, S.; Bansil, R.; Konak, C. *Macromolecules* **1993**, *26*, 305−312.
(14) Camins, B. C.; Russo, P. S. *Langmuir* **1994**, *10*, 4053−4059.
(15) Sohn, D.; Russo, P. S.; Davila, A.; Poché, D. S.; McLaughlin, M. L. *J. Colloid Interface Sci.* **1996**, *177*, 31−44.
(16) Akcasu, A. Z.; Nagele, G.; Klein, R. *Macromolecules* **1991**, *24*, 4408−4422.
(17) Phillies, G. D. J. *J. Chem. Phys.* **1974**, *60*, 983−989.
(18) Fraden, S.; Maret, G.; Caspar, D. L. D. *Phys. Rev. E* **1993**, *48*, 2816−2837.
(19) Boedtker, H.; Simmons, N. S. *J. Am. Chem. Soc.* **1958**, *80*, 2550−2557.
(20) Butler, P. J.; Klug, A. *Sci. Am.* **1978**, 62−69.
(21) Smit, J. A. M.; van Dijk, J. A. P. P.; Mennen, M. G.; Daoud, M. *Macromolecules* **1992**, *25*, 3585−3590.
(22) Senti, F. R.; Hellman, N. N.; Ludwig, N. H.; Babcock, G. E.; Tobin, R.; Glass, C. A.; Lamberts, B. L. *J. Polym. Sci.* **1955**, *17*, 527−546.

(23) Wada, A.; Suda, N.; Tsuda, T.; Soda, K. *J. Chem. Phys.* **1969**, *50*, 31−35.
(24) Berne, B.; Pecora, R. *Dynamic Light Scattering*; Wiley: New York, 1976; Chapter 8.
(25) Aragon S., S. R.; Pecora, R. *J. Chem. Phys.* **1985**, *82*, 5346−5353.
(26) Flamberg, A.; Pecora, R. *J. Phys. Chem.* **1984**, *88*, 3026−3033.
(27) Zero, K.; Pecora, R. *Macromolecules* **1982**, *15*, 87−93.
(28) Wilcoxon, J.; Schurr, J. M. *Biopolymers* **1983**, *22*, 849−867.
(29) Rallison, J. M.; Leal, L. G. *J. Chem. Phys.* **1981**, *74*, 4819−4826.
(30) Tracy, M. A.; Pecora, R. *Annu. Rev. Phys. Chem.* **1992**, *43*, 525−557.
(31) Maeda, T. *Macromolecules* **1990**, *23*, 1464−1474.
(32) *Commonwealth Mycological Institute, Association of Applied Biologists Descriptions of Plant Viruses*; Farnham Royal: Slough, England, 1975.
(33) Russo, P. S.; Saunders, M. J.; DeLong, L. M.; Kuehl, S. K.; Langley, K. H.; Detenbeck, R. W. *Anal. Chim. Acta* **1986**, *189*, 69−87.
(34) DeLong, L. M.; Russo, P. S. In *ACS Advances in Chemistry Series #227*; Provder, T., Craver, C., Eds.; American Chemical Society: Washington, DC, 1990; Chapter 5.
(35) Steere, R. L. *Science* **1963**, *140*, 1089−1090.
(36) King, T. A.; Knox, A.; Mc Adam, J. D. G. *Biopolymers* **1973**, *12*, 1917−1926.
(37) Provencher, S. W. *Comput. Phys.* **1982**, *27*, 213−227.
(38) Provencher, S. W. *Comput. Phys.* **1982**, *27*, 229−242.
(39) Stepanek, P. In *Dynamic Light Scattering, The Method and Some Applications*; Brown, W., Ed.; Clarendon Press: Oxford, U.K., 1993; pp 175−241.
(40) Koppel, D. E. *J. Chem. Phys.* **1972**, *57*, 4814−4820.
(41) Broersma, S. *J. Chem. Phys.* **1960**, *32*, 1626.
(42) Broersma, S. *J. Chem. Phys.* **1960**, *32*, 1632.
(43) Broersma, S. *J. Chem. Phys.* **1981**, *74*, 6989.
(44) Russo, P. S. In *Dynamic Light Scattering, the Method and Some Applications*; Brown, W., Ed.; Oxford: New York, 1993; pp 512−553.
(45) Tirado, M. M.; Martinez, C. L.; de la Torre, J. G. *J. Chem. Phys.* **1984**, *81*, 2047.
(46) Van Holde, K. E. *Physical Biochemistry*; Prentice-Hall, Inc.: Englewood Cliffs, NJ, 1985; Chapter 5.
(47) Lauffer, M. A. *J. Am. Chem. Soc.* **1944**, *66*, 1188−1194.
(48) Doi, M.; Edwards, S. F. *The Theory of Polymer Dynamics*; Clarendon Press: Oxford, U.K., 1986; Chapter 9.
(49) Doi, M.; Edwards, S. F. *J. Chem. Soc., Faraday Trans 2* **1978**, *74*, 560−570.
(50) Doi, M.; Edwards, S. F. *J. Chem. Soc., Faraday Trans 2* **1978**, *74*, 918−932.
(51) Deggelmann, M.; Graf, C.; Hagenbuchle, M.; Hoss, U.; Johner, C.; Kramer, H.; Martin, C.; Weber, R. *J. Phys. Chem.* **1994**, *98*, 364−368.
(52) Chu, B. *Laser Light Scattering*; Academic Press: New York, 1991; Chapter 8.
(53) Sohn, D.; Russo, P. S.; Roitman, D. B. *Ber. Bunsen-ges. Phys. Chem.* **1996**, *100*, 821−828.
(54) Flory, P. J. *Macromolecules* **1978**, *11*, 1138−1141.
(55) Cotts, P. M.; Berry, G. C. *J. Polym. Sci.* **1983**, *21*, 1255−1274.
(56) A photomultiplier tube with a small photocathode was used without a diffusing element; beam wander can produce some drift in this case.
(57) Won, J.; Onyenemezu, C.; Miller, W. G.; Lodge, T. P. *Macromolcules* **1994**, *27*, 7389−7396.
(58) Ullmann, G. S.; Ullmann, K.; Lindner, R. M.; Phillies, G. D. J. *J. Phys. Chem.* **1985**, *89*, 692−700.
(59) deGennes, P. G. *Scaling Concepts in Polymer Physics*; Cornell University Press: Ithaca, NY, 1979; Chapter 3.
(60) Phillies, G. D. J. *Macromolecules* **1986**, *19*, 2367−2376.
(61) Martin, J. E. *Macromolecules* **1986**, *19*, 922−925.
(62) Phillies, G. D. J. *J. Phys. Chem.* **1992**, *96*, 10061−10066.
(63) Bu, Z.; Russo, P. S.; Tipton, D. L.; Negulescu, I. I. *Macromolecules* **1994**, *27*, 6871−6882.
(64) Tinland, B.; Maret, G.; Rinaudo, M. *Macromolecules* **1990**, *23*, 596−602.
(65) deGennes, P. G. *J. Phys. (Paris)* **1981**, *42*, 473−477.
(66) Pecora, R.; Deutch, J. M. *J. Chem. Phys.* **1985**, *83*, 4823−4824.
(67) Bawden, F. C.; Pirie, N. W.; Bernal, J. D.; Fankuchen, I. *Nature* **1936**, *138*, 1051−1052.

MA970032F